Engineering 3 (2017) 244–256

Contents lists available at ScienceDirect

Engineering

journal homepage: www.elsevier.com/locate/eng

Research
Smart Process Manufacturing—Article

Interactions between the Design and Operation of Shale Gas Networks, Including CO_2 Sequestration

Sharifzadeh Mahdi *, Xingzhi Wang, Nilay Shah

Center for Process Systems Engineering, Department of Chemical Engineering, Imperial College London, London SW7 2AZ, UK

ARTICLE INFO

Article history:
Received 31 December 2016
Revised 13 February 2017
Accepted 20 February 2017
Available online 1 April 2017

Keywords:
Shale gas
Hydraulic fracturing
Scheduling
Well shut-in
CO_2 sequestration
Simultaneous optimization

ABSTRACT

As the demand for energy continues to increase, shale gas, as an unconventional source of methane (CH_4), shows great potential for commercialization. However, due to the ultra-low permeability of shale gas reservoirs, special procedures such as horizontal drilling, hydraulic fracturing, periodic well shut-in, and carbon dioxide (CO_2) injection may be required in order to boost gas production, maximize economic benefits, and ensure safe and environmentally sound operation. Although intensive research is devoted to this emerging technology, many researchers have studied shale gas design and operational decisions only in isolation. In fact, these decisions are highly interactive and should be considered simultaneously. Therefore, the research question addressed in this study includes interactions between design and operational decisions. In this paper, we first establish a full-physics model for a shale gas reservoir. Next, we conduct a sensitivity analysis of important design and operational decisions such as well length, well arrangement, number of fractures, fracture distance, CO_2 injection rate, and shut-in scheduling in order to gain in-depth insights into the complex behavior of shale gas networks. The results suggest that the case with the highest shale gas production may not necessarily be the most profitable design; and that drilling, fracturing, and CO_2 injection have great impacts on the economic viability of this technology. In particular, due to the high costs, enhanced gas recovery (EGR) using CO_2 does not appear to be commercially competitive, unless tax abatements or subsidies are available for CO_2 sequestration. It was also found that the interactions between design and operational decisions are significant and that these decisions should be optimized simultaneously.

1. Introduction

Dwindling petroleum reservoirs have stimulated new research into the commercialization of unconventional resources such as shale gas. Unlike natural gas, its conventional counterpart, shale gas needs to be extracted from ultra-low-permeability geological formations. Therefore, special methods such as horizontal drilling, hydraulic fracturing, carbon dioxide (CO_2) injection, and shut-in operations are required to improve the economic benefits. The decisions involved are highly complex and can be broadly categorized into design and operational decisions. The common feature of design decisions is their immediate realization at an early stage of shale gas exploration. Examples include the number of wells and their spacing and length, and the number of fractures and their distance. It is said that design decisions are "here-and-now" decisions. By comparison, operational decisions such as production rate, shut-in scheduling, and potential CO_2 injection are made only at later stages and during shale gas extraction. The methodology by which the interactions between design and operational decisions are considered is known as "integrated design and control" [1–3].

The design of shale gas networks has been the focus of several researchers. Ran and Kelkar [4] studied the economic implications of the number of fracture stages. They indicated that, as the number of fracture stages increases, the cost of completion becomes a major cost contributor; beyond a certain number of fractures, the cost increases do not cover the incremental benefits. Balan et al. [5]

* Corresponding author.
E-mail address: mahdi@imperial.ac.uk

http://dx.doi.org/10.1016/J.ENG.2017.02.007

applied a proxy model to optimize the well spacing, hydraulic fracture spacing, and half-length in a hypothetical shale gas reservoir, and made similar observations.

In parallel, the operation of shale gas production networks has been the focus of other researchers. Compared with their conventional counterparts, shale gas reservoirs experience sharp pressure depletions and potential liquid loading that can greatly influence the gas production rate. Appropriate shut-in operations can avoid this problem and increase gas extraction [6]. Knudsen [7] incorporated shut-in decisions into an optimization procedure for a single well, with different shut-in time cycles in four examples. The results revealed that shale gas production losses can be greatly reduced using shut-in procedures. Later, Knudsen et al. [8] introduced a scheme for multi-well shale gas well scheduling. A single-layered and radical composite proxy model for reservoirs was built, and mixed-integer linear programming (MILP) was applied. Unfortunately, the model showed discrepancies from actual complex systems for predicting shut-in operations. To enhance the performance of their models, Knudsen and Foss [9] established a new proxy model for shale gas wells based on partial differential equations. A generalized disjunctive program (GDP) was also applied to incorporate well shut-in arrangements. Later, Knudsen et al. [10] built a scheme for a multi-well shut-in arrangement using a three-region proxy model with reasonable accuracy. They applied a Lagrangian relaxation method for system optimization.

Shut-in procedures can be applied to a large range of conditions. However, they may result in undesirable interruptions in long-term production. Injecting CO_2 into a shale gas reservoir is an alternative method to enhance shale gas recovery. Shale formations preferentially adsorb CO_2 (about 5–10 times more than methane, CH_4 [11]), which can lead to an increase in shale gas recovery. Intensive studies are underway to gain better understanding and improve the performance of shale gas recovery using gas injection methods. Eshkalak et al. [12] compared the performance of shale gas recovery using CO_2 injection and re-fracturing. A dual porosity and permeability model was built for both scenarios. The results illustrated that re-fracturing performs better than gas injection due to the formation of new drainage areas. However, gas injection performance increased shale gas extraction in long-term scenarios. It was also found that using a gas injection method after re-fracturing is very effective for enhancing shale gas recovery. Researchers at the National Energy Technology Laboratory (NETL) [13] applied a numerical simulation method to simulate shale gas recovery using a CO_2 injection method. They built a dual porosity and permeability model to evaluate shale gas recovery performance under different CO_2 injection rates. The results showed that a low gas injection rate can be more economical due to lower operational costs. In addition, a high gas injection rate may create undesired fractures. Li and Elsworth [14] applied modeling of Barnett shale in order to estimate shale gas recovery under different pressures. The results revealed that production of CH_4 was increased by 2.3%, 14.3%, and 28.5% when CO_2 was injected at 0 MPa, 4 MPa, and 8 MPa, respectively. In conclusion, CO_2 injection is an efficient technique to improve shale gas recovery; in addition, this technique sequesters a greenhouse gas (GHG).

While a thorough review of the research in the field is not the focus of the present contribution, based on the aforementioned critical analysis, it is immediately evident that shale gas network design and operational decisions are drastically different and more challenging than their natural gas counterparts. In particular:

- Both design and operational decisions have significant economic implications;
- Both design and operational decisions are highly nonlinear, and do not lend themselves to conventional simplifications; and
- Design and operational decisions differ in that the former are made at much earlier stages, although both are highly interactive and interdependent.

With the aim of gaining in-depth insight into the decisions involved in the design and operation of shale gas networks, the present research develops a full-physics model of a shale gas network, consisting of four production and four injection wells. This rigorous model is then applied to a comprehensive sensitivity analysis in which design decisions such as the number of fractures in each well, fracture distance, well length, and the arrangement of production and injection wells, and operational decisions such as the possibility of CO_2 injection and shut-in scheduling (timing, durations, and frequency) are comprehensively studied. Using an example, we also demonstrate that design and operational decisions are highly interactive and require simultaneous decision-making. The paper concludes by proposing a future research direction.

2. Full-physics model of a shale gas reservoir

A full-physics model was established using numerical simulation software (Eclipse). As a shale gas reservoir is an unconventional reservoir, the coal-bed methane (CBM) method, which is especially programmed for unconventional gas reservoirs, was selected. Non-Darcy flow and instant desorption were assumed. In order to simulate the matrix-fracture system of a shale gas reservoir, a dual-porosity and dual-permeability model was constructed using the Eclipse simulation software tool. Unlike the single-permeability model, in which the matrix blocks are linked only through the fracture system and the matrix blocks act as sources, a dual-permeability system has flow occurring directly between neighboring matrix blocks. In order to simulate the hydraulic fractures, local grid refinement (LGR) was applied and the porosity and permeability of certain blocks were adjusted to the fracture's porosity and permeability.

In a fractured shale gas reservoir, fluids exist in two systems that are connected with each other:

- The rock matrix, which occupies most of the reservoir volume; and
- The rock fractures, which are highly permeable.

In shale gas reservoirs, the rock matrix has high porosity and low permeability, while the rock fractures feature low porosity and high permeability [15]. Soeder [16] suggested the average rock matrix porosity to be about 10%, and Wang and Wu [17] estimated the fracture porosity to be about 1%. The permeability of the shale gas matrix can be calculated by the Klinkenberg correlation [18]:

$$K = k^{\infty} \times \left(1 + \frac{b_k}{\overline{P}}\right) \tag{1}$$

where b_k is the Klinkenberg coefficient; $\overline{P}$ is the mean pore pressure; and k^{∞} is the reference permeability. Aguilera [19] postulated a simplified empirical equation based on shale gas reservoirs:

$$r = 2.665\left(\frac{k_m}{100\phi_m}\right)^{0.45} \tag{2}$$

where r is the pore size, and ϕ_m and k_m are the porosity and permeability in the matrix, respectively. In the research study presented in this paper, the value of 0.1 for ϕ_m and the value of 6 nm for r were considered. Liu et al. [20] measured the average pore size as 5.97 nm using gas adsorption, and used mercury intrusion techniques to obtain the value of 60.7 nd (1 nd = 9.869233×10^{-10} μm^2) for permeability. Cho et al. [21] suggested the permeability of hydraulic fractures to be around 100 000 md. Hydraulic or primary fractures are those that are induced by the injection of hydraulic fracturing fluid. They are propagated in the direction of least principal stress [6]. Proppants provide high permeability for these types of fractures [7] and enable the easy flow of gas from the matrix to the wells. By comparison, secondary fractures are the result of geomechanical changes in the rock, induced by hydraulic fractures [7]. Ozkan

et al. [22] investigated the permeability of secondary fractures. In the initial conditions, the pressure was found to be 5000 psi (1 psi = 6.894757 × 10^3 Pa) and the permeability to be 2000 md. During the extraction process, the permeability of the secondary fractures induced by hydraulic fractures was found to be around 200 md, since the flowing bottom hole pressure dropped to about 750 psi. The permeability of the natural fractures was deemed to be negligible, as it has little effect on productivity; the limiting factor is the flow capacity of the matrix [22]. Desorption can be modeled using the Langmuir equation:

$$V_{ads} = \frac{V_L p}{p_L + p} \tag{3}$$

where V_{ads} represents the volume of gas adsorbed in the reservoir rock, with a unit of scf·t^{-1} (scf is short for standard cubic foot, 1 scf = 0.0283168 m^3); p is the pressure; and V_L and p_L are the Langmuir volume and Langmuir pressure, respectively. The Langmuir volume is the maximum adsorption capacity of the rock and the Langmuir pressure is the pressure at which V_{ads} is equal to half of the Langmuir volume. The so-called "instant desorption" model can be applied when the desorption process is negligible. Queipo et al. [23] investigated the storage capacity of a specific shale gas reservoir. Using Langmuir isotherm properties, both free and adsorbed gas can be plotted as a function of pressure. At an initial pressure of 5000 psi [24–26], the gas content in the reservoir is approximately 70% free gas and 30% adsorbed gas. As the reservoir pressure drops toward the flowing bottom hole pressure (FBHP) of 750 psi, this ratio shifts to 60% adsorbed gas, and the content of adsorbed gas remains almost unchanged. It is evident that gas desorption will not significantly affect shale gas production until the reservoir inventory has decreased substantially below the initial pressure. This behavior is consistent with the observations made in a previous work on the Barnett shale [27], in which gas desorption appeared in the decline curve after significant production but had only a minor effect on cumulative gas production. Thus, the desorption of shale gas is negligible and the instant desorption model can be applied. The adsorption-desorption process is represented as a source term in the matrix pore system.

The fluid flow in the shale gas reservoir can be divided into two parts:

- Gas flow toward the fractures within the pore space of the matrix; and
- Gas flow in the fractures.

For gas flow within the matrix, the flow rate is very small. Thus, the gas flow follows Darcy's law. For gas flow in the fractures, the flow is non-Darcy flow due to high velocity; it can be correlated using the Forchheimer correction, which takes the inertia effects into account [28,29]:

$$-\frac{\mathrm{d}p}{\mathrm{d}x} = \frac{\mu}{K} v + \rho \beta v^2 \tag{4}$$

where dp/dx is the pressure gradient; v is the gas velocity; μ is the fluid viscosity; K is the effective permeability of rock; ρ is the fluid density; and β is the non-Darcy coefficient in 1 ft^{-1} (1 ft = 0.3048 m). A general form of the non-Darcy coefficient is expressed below [28]:

$$\beta = aK^{-b} \tag{5}$$

where a and b are constants determined by laboratory experiments; their estimated values are 109 for a and 1 for b.

The main body of the reservoir is occupied by stimulated reservoir volume (SRV). Hydraulic fractures and induced secondary fractures penetrate throughout this volume. The matrix permeability of the SRV part is complex, and is different from the part outside the SRV. The average matrix permeability of SRV at the beginning of shale gas extraction is 3 md [29]. Since the aperture of the fracture is much smaller than the dimensions of the blocks, an average permeability of the whole area around the fracture should be considered. Table 1 [30] summarizes the important parameters of the simulation model that were applied for modeling primary and secondary fractures.

Table 1
Parameters of the simulation model.

Parameter	Value
Dimensions of the field (m)	205 × 205 × 99
Number of cells in x, y, and z directions	41 × 41 × 11
Matrix porosity	10%
Hydraulic fracture porosity	1%
Matrix permeability (nd)	60.7
Hydraulic fracture permeability (md)	100 000
Secondary fracture permeability (md)	200
Fracture block permeability (md)	100 [30]
Fracture half-length (m)	25 [30]

In order to manage the computation time in the present study, a small-scale SRV was considered; this can be thought of as a segment of a densely explored reservoir. The field dimensions were 205 m × 205 m in the horizontal plane and 99 m in depth. The number of blocks in the simulation model were 41 × 41 × 11, and the dimensions of each block in the x, y, and z directions were 5 m, 5 m, and 9 m, respectively. Fig. 1 shows grid networks with hydraulic fractures. The production and injection wells are specified by the letters P and I, respectively. The injection wells are vertical, and the production wells have a vertical segment followed by a horizontal one.

In our case, we wish to explore the possibility of CO_2 injection as well. Hence, we consider the CO_2 component in addition to CH_4. A compositional model (Eclipse 300 [29]) was applied in order to satisfy the desired case. A multi-well pad that consists of four orthogonal production wells was considered in the model. In addition, four injection wells are in operation when the CO_2 injection is applied. The production wells and injection wells are arranged in two ways, as shown in Fig. 2. In the alpha arrangement, the injection wells are at a 45° angle to each of the production wells. By comparison, in the beta arrangement, the injection wells and the corresponding production wells are adjacent to each other.

The objective function that we seek to optimize is the net present value (NPV) of the field development, which is the sum of the discounted cash flows (DCFs) minus the capital expenditures C_{cap}:

$$NPV = \sum_{n=1}^{N} DCF_n - C_{cap} \tag{6}$$

The capital costs are the sum of the leasing cost, drilling cost, fracturing cost, and CO_2 injection cast [30]:

$$C_{cap} = C_{lease} + C_{drill} + C_{frac} + C_{injection} \tag{7}$$

It is estimated that the cost of drilling and completing a well in the Woodford shale (Oklahoma), where the shale is 6000–11 000 ft deep, is 6.7 million USD, whereas the cost of drilling and completing a new well in the Haynesville shale is estimated to be 9.5 million USD [31]. According to the more scalable data provided by Wilson and Durlofsky [32], the drilling cost is 250 USD·ft^{-1}, the completing (fracturing) cost is 21 750 USD·$stage^{-1}$, and the leasing cost is set at 11 130 USD for the field. According to the work of Allinson et al. [33], the CO_2 injection cost is 1000 AUD·t^{-1}, which is approximately 1.49 USD·m^{-3}. This cost includes CO_2 compression, transport, and injection. A discounted cash-flow function for shale gas was applied [34]:

$$DCF_n = (1-T)(q_n G - C_{LOE} \times t)(1+i)^{-n} \tag{8}$$

where q_n is production over the time step; G is the gas price; T is the

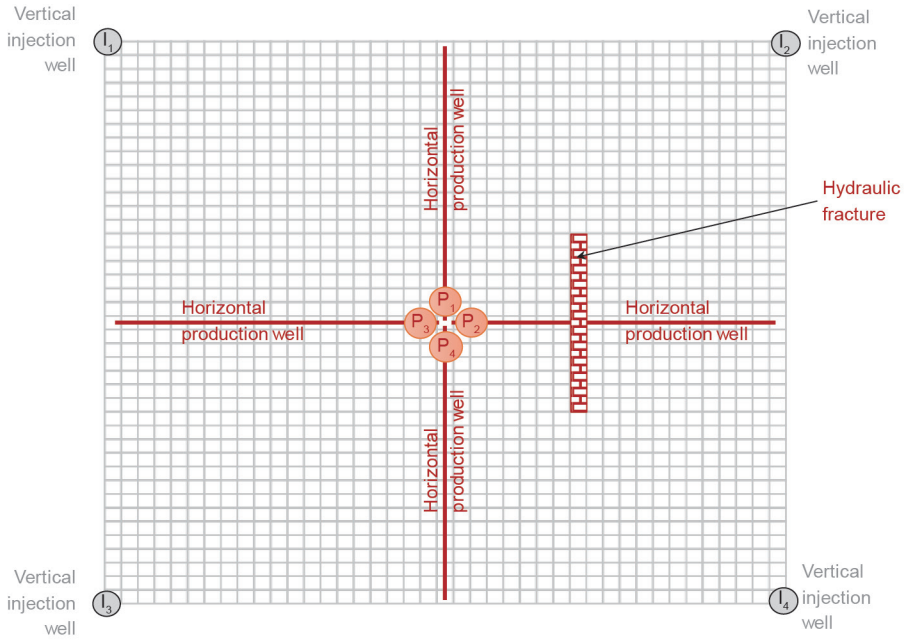

Fig. 1. Grid networks of the shale gas model (alpha arrangement).

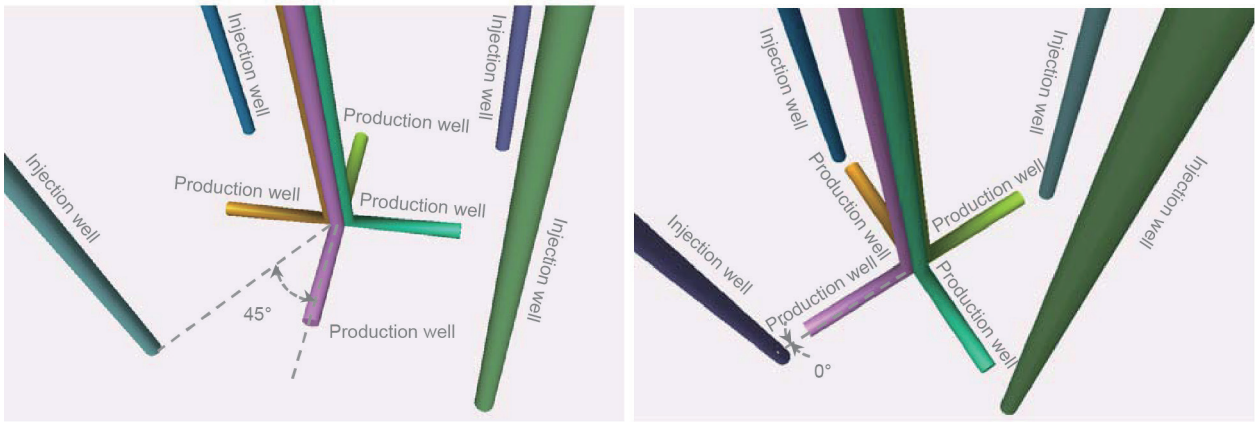

Fig. 2. (a) Well arrangement (alpha): 45° angle between production and injection wells; (b) well arrangement (beta): 0° angle between production and injection wells.

tax rate; i is the discount rate; and C_{LOE} is the lease operating cost, which is the costs of the equipment used during the extraction work.

Shale gas price is affected by the same factors that influence conventional gas prices; hence we applied a conventional gas price to the shale gas project. The gas price of 9.55 USD·MMBtu^{-1} [31] was used for this study, where MMBtu stands for one million British thermal units. Other parameters can be found in Table 2 [30].

Gas production can be shown in a time step that also considers shut-in operation, as follows:

$$q_n = \int_{t_n}^{T_1} r(t)\,\mathrm{d}t + \sum_{i=2}^{m-1}\left[\int_{T_i'}^{T_i} r(t)\,\mathrm{d}t + \int_{T_i'}^{T_{i+1}} r(t)\,\mathrm{d}t\right] + \int_{T_m'}^{t_{n+1}} r(t)\,\mathrm{d}t \qquad (9)$$

where $r(t)$ is gas production rate; m refers to shut-in periods in a time step; T_i and T_i' are the start and end times of each shut-in interval, respectively; and $T_i' - T_i$ is the shut-in interval. The gas production rate r can be defined as follows [31]:

$$r = r_{\mathrm{i}}\left(1 + \eta D_{\mathrm{i}} t\right)^{-\frac{1}{\eta}} \qquad (10)$$

where r is the production rate at time t, with a unit of Mcf·a^{-1} (Mcf is short for thousand cubic feet); r_{i} is the initial production rate at time t = 0; and D_{i} and η are constants, such that D_{i} is the initial rate of decline in production and η is the rate of change in D_{i} over time. Lake et al. [31] provided the values of these parameters: r_{i} (initial production rate at time 0) = 19 500 Mcf·d^{-1}, D_{i} (initial rate of decline in production) = 85% for the first year, and η (the rate of change in D_{i}) = 1.0.

Table 2
Other parameters in DCF function.

Parameter	Value
Tax rate	30%
Lease operating cost	25 USD·d^{-1}
Discount rate	15%

3. Sensitivity analysis

As a complex process, shale gas extraction contains a large number of decisions that can influence the gas production and drilling efficiency. It is essential to screen out the decisions that have a

great impact on shale gas production. An effective method of doing so is to change one factor by steps, while keeping other decisions unchanged. To reduce the workload, we selected some typical parametric values as the baseline for the analysis, and then screened the most sensitive decisions accordingly. Two types of decisions can be immediately identified: design decisions and operational decisions. These are discussed below.

3.1. Design decisions

Design decisions can greatly influence gas production. Once the shale gas extraction comes into operation, the network design is fixed and there is little or no room to revise these decisions. Several crucial design decisions, including the number of fractures in each well, fracture distance, well length, and well arrangement, are considered here.

3.1.1. Number of fractures in each well

Hydraulic fracturing is indispensable in the shale gas extraction process, due to the ultra-low permeability of shale reservoirs. The number of hydraulic fractures in each well will have a great impact on shale gas production. As the SRV area used in this study is not very large (205 m × 205 m × 99 m), a case with one fracture, a case with two fractures, and a case with three fractures were considered. The fracture distances are even, and the total well length is 100 m. Wells are positioned in the alpha arrangement. CO_2 injection and shut-in operations are not considered in this operation.

Fig. 3(a) shows the production rate of the three cases. It can be seen that the production rate increases significantly at the beginning with an increasing number of fractures. On the third day, the gas production rate of the case with three fractures is more than twice the rate of the case with only one fracture per well. This observation can be explained by the high permeability of hydraulic fractures and induced secondary fractures. Hydraulic fractures have very high permeability compared with the shale gas matrix. The fractures can penetrate the tight rock of the shale and release trapped shale gases. Secondary fractures are also induced by hydraulic fractures, and release additional shale gas. Having more fractures means that it is easier for the shale gas to move from the matrix to the well. Thus, the gas production rate initially increases when the fracture number increases. It was also observed that the gas production rate drops more sharply when there are more fractures. This result is due to the influence of pressure drop. When there are more fractures, shale gas will be released from the shale gas reservoir more quickly, and the pressure of the matrix will decrease more quickly as well. As a consequence, the extraction rate of shale gas will decrease more quickly. Therefore, there is a trade-off between the total amount of gas produced and the number of fractures. Fig. 3(b) illustrates the total gas production. The result shows that the case with two fractures has the highest total shale gas production, while the case with one fracture has only a narrow advantage compared with the case with three fractures. Although the case with three fractures has the highest production rate at the beginning, it has the lowest total gas production, due to the sharp drop in gas production rate that occurs later in the process. Table 3 shows the NPV of the three scenarios. When economic benefits are taken into account, the case with two fractures on each well is the most profitable. Although this arrangement requires more investment than the case with one fracture, the additional costs result in superior profits. It was also found that the case with three fractures has a negative economic performance, due to the high costs of fracturing.

3.1.2. Fracture distance

The formation of secondary fractures is very complex and is greatly influenced by the distance between fractures. Different fracture distances can form different secondary fracture structures and thus influence the shale gas production. In this study, three fracture distances are taken into account: 20 m, 30 m, and 45 m. Each case has two fractures, and the well length is 100 m. Wells are positioned in the alpha arrangement, and no CO_2 injection or shut-in operation is applied. Fig. 4 shows the pressure map of the shale gas reservoir for different fracture distances on the 15th day of extraction.

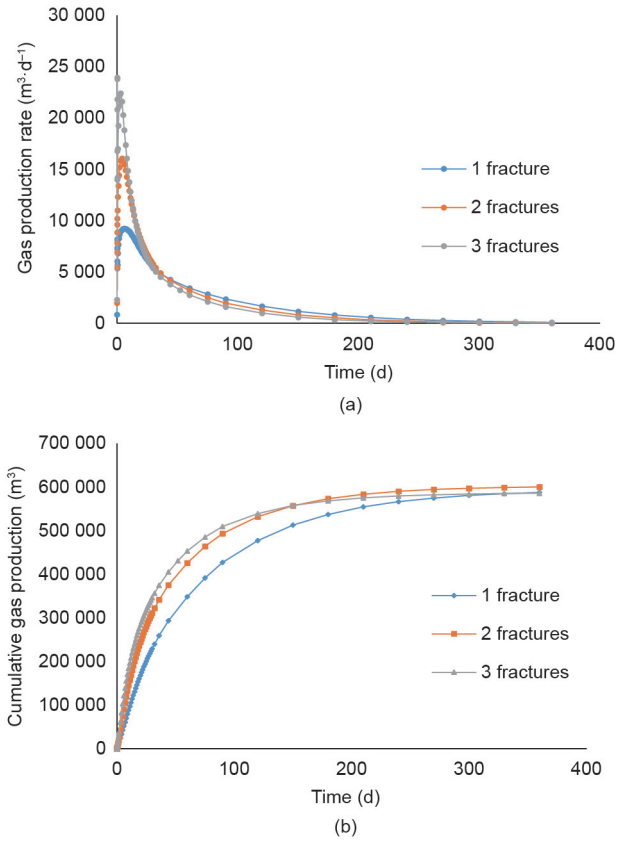

Fig. 3. (a) Shale gas production rate for different numbers of fractures; (b) total gas production for different numbers of fractures.

Table 3
NPV of shale gas production for different numbers of fractures.

Fracture number	NPV (USD)
1	21 090
2	21 563
3	Negative

Fig. 5(a) shows the gas production rates for different fracture distances. Fig. 5(b) shows the cumulative production for the corresponding scenarios. Although the differences are incremental, it suggests that the case with a 30 m fracture distance has the highest total gas production. The implication is that if the distance between fractures is too large or too small, then the secondary fractures induced by the hydraulic fractures cannot reasonably cover the whole reservoir; and that the secondary fracture structure created in this case is better than those created in other cases. This implication can also be observed from the pressure map, as the case with a 30 m fracture distance, shown in Fig. 4(b), provides a larger and more homogeneous low-pressure area that indicates better gas release. Table 4 lists the NPV for different fracture distances. The case with a 30 m distance has the highest shale gas production and the greatest economic benefits.

3.1.3. Well length

Well length is an important design factor that must be consid-

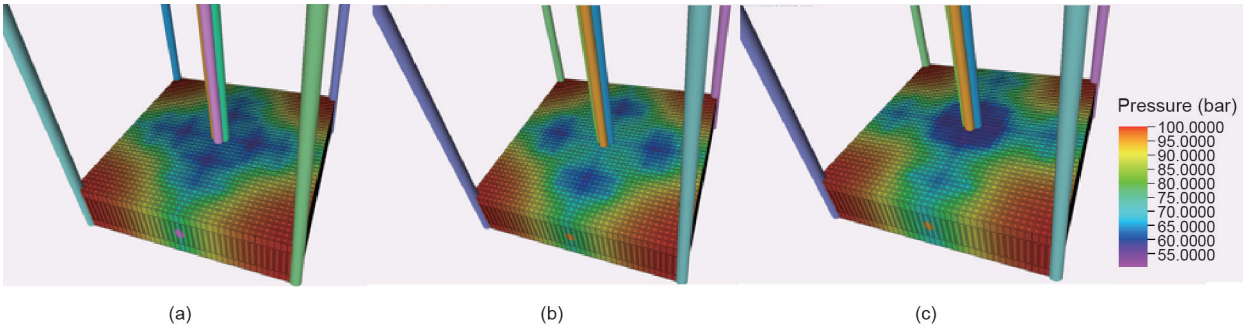

Fig. 4. The fracture/matrix pressure map for different fracture distances on the 15th day. (a) 20 m; (b) 30 m; (c) 45 m. 1 bar = 100 kPa.

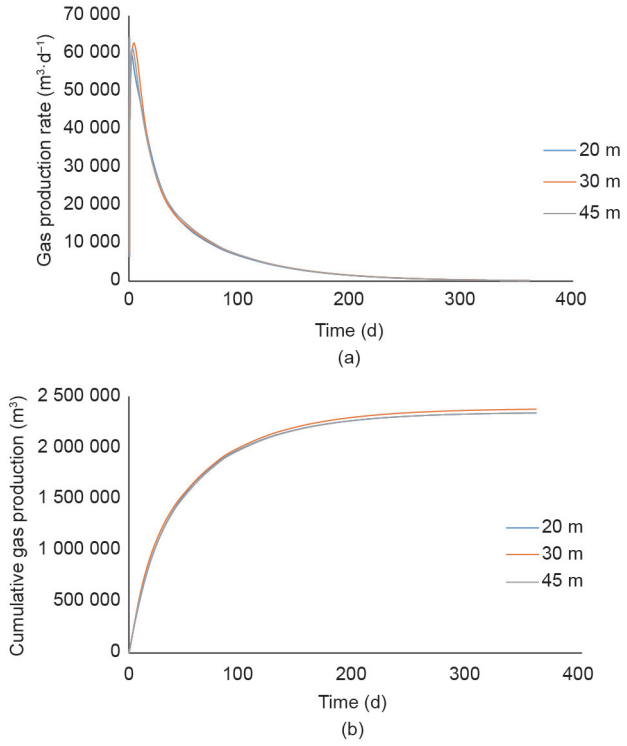

Fig. 5. (a) Shale gas production rate for different fracture distances; (b) total production rate for different fracture distances.

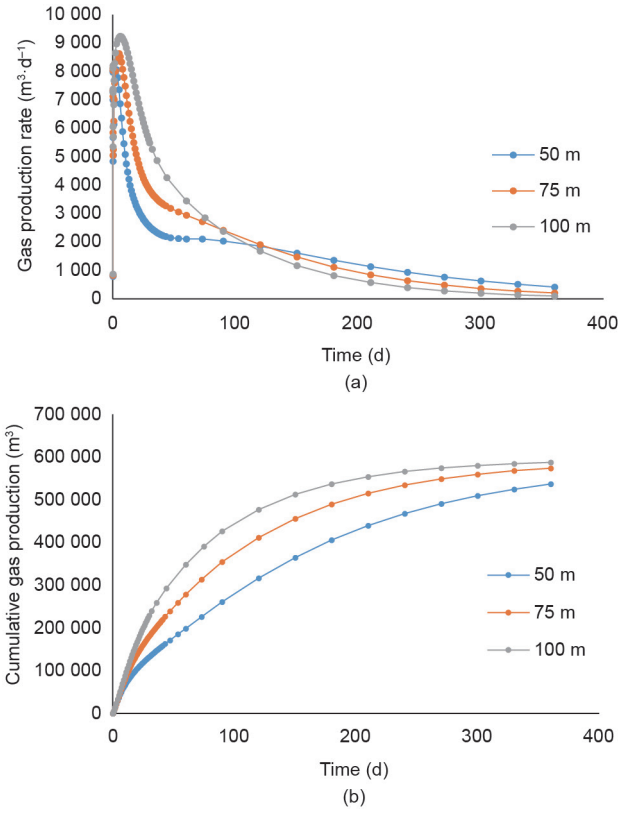

Fig. 6. (a) Shale gas production rate for different well lengths; (b) total gas production for different well lengths.

Table 4
NPV of shale gas production for different fracture distances.

Distance between fractures (m)	NPV (USD)
20	18 292
30	21 563
45	19 771

Table 5
NPV of shale gas production for different well distances.

Well length (m)	NPV (USD)
50	51 693
75	38 854
100	21 090

ered. In the present study, lengths of 50 m, 75 m, and 100 m were considered for the sensitivity analysis. In these scenarios, each well has only one fracture, and wells are positioned in the alpha arrangement. There is no CO_2 injection or shut-in operation.

As can be seen in Fig. 6(a), the longer well has a higher gas production rate at the beginning, but its pressure decrease is sharper. If the well is longer, more gas will permeate from the matrix to the well via the well wall. Fig. 6(b) shows the cumulative shale gas production. The total gas production increases with the increase of well length.

Table 5 shows the NPV for different well distances. When economic benefit is taken into account, the cost of drilling a well is a very important factor to consider. After calculation, the case with a 50 m well length has the highest NPV, and the NPV decreases as the well length increases. This is contrary to the result regarding total gas production, which means that the cost of well drilling plays an important role in the shale gas extraction process.

3.1.4. Well arrangement

When the CO_2 injection method is applied to improve shale gas production, the arrangement of the production wells and injection wells can influence gas quality and production. Two well arrangements were considered in this study, as shown in Fig. 2(a) and Fig. 2(b). In the alpha arrangement, each injection well is at a 45° angle to the closest production well. In the beta arrangement, the

horizontal part of each production well heads toward the nearest injection well. Keeping other decisions fixed, at two fractures for each well and a well length of 75 m, we applied CO_2 injection with an injection rate of 7079.2 $m^3 \cdot d^{-1}$. No shut-in operation was in place.

Fig. 7(a) shows the gas production rates of various scenarios for different well arrangements, while Fig. 7(b) illustrates the mole fractions of the extracted gas. Fig. 7(c) shows the cumulative gas production of the two cases. The result can be divided into three phases. In the first phase, the production gas does not contain any CO_2. The curve of the gas production rate is similar to that without CO_2 injection. In the second phase, the mole fraction of CO_2 begins to increase while the mole fraction of CH_4 simultaneously begins to decrease. The production rate of shale gas shows an increase in this period. In the last phase, the mole fractions of the components become stable and the shale gas production rate slowly decreases. It can also be observed from the result that phase one is short and phase two is entered into more quickly in the beta arrangement, as compared with the alpha arrangement. This result is caused by the distance and angle between the injection wells and hydraulic fractures. The hydraulic fractures in the beta arrangement are closer to the injection wells than those in the alpha arrangement, and the CO_2 flow is almost vertical to the hydraulic fractures, which makes it easier for CO_2 to "break through" the production wells. The total CH_4 production can be estimated by multiplying the shale gas mole fraction by the production rate and integrating over the time horizon. The resulting total CH_4 production is 530 756 m^3 in the alpha arrangement and 423 804 m^3 in the beta arrangement. Although the beta arrangement has a higher total gas production, the alpha arrangement extracts more CH_4. This result indicates that the quality and quantity of shale gas production will decrease if injected CO_2 moves into the production well too quickly. The direction of and distance between the injection well and the production well are crucial design decisions.

3.2. Operational decisions

Operational decisions can influence shale gas production and are flexible to deal with potential uncertainties. CO_2 injection and well shut-in operations are efficient approaches to enhance shale gas production rates. It is essential to study their impacts on shale gas production.

3.2.1. CO_2 injection

CO_2 injection is an efficient way to improve shale gas production, and can also act as a carbon sequestration method. The injected CO_2 can push the shale gas in the matrix toward the production wells, thus enhancing shale gas production. However, it is important to control the injection rate, since too-high injection rates can decrease the quality of the produced shale gas due to the channeling effect. In this section, we take six CO_2 injection rates into account: 0 $m^3 \cdot d^{-1}$, 50 $m^3 \cdot d^{-1}$, 100 $m^3 \cdot d^{-1}$, 300 $m^3 \cdot d^{-1}$, 3000 $m^3 \cdot d^{-1}$, and 7079.2 $m^3 \cdot d^{-1}$. Each well has two fractures, and the fracture distances are even. Wells are arranged in the alpha formation without shut-in operation.

Fig. 8(a) reveals the shale gas production rates of the six investigated cases. When the CO_2 injection rate increases, the decline in the gas production rate slows down. When the CO_2 injection rate reaches 3000 $m^3 \cdot d^{-1}$, the gas production rate becomes stable after 60 d and even increases slightly for the CO_2 injection rate of 7079.2 $m^3 \cdot d^{-1}$. The CO_2 breakthrough into the production wells increases the quantity of the produced gas. Fig. 8(b) illustrates the total gas production of the considered scenarios. Fig. 8(c) gives more detail in terms of the shale gas (CH_4) mole fraction in the extracted gas. It is clear that CO_2 enters the production well earlier and faster as the injection rate increases. The results suggest that injection rates of 50 $m^3 \cdot d^{-1}$ and 100 $m^3 \cdot d^{-1}$ lead to an increase in high-quality shale gas. In contrast, the cases with 3000 $m^3 \cdot d^{-1}$ and 7079.2 $m^3 \cdot d^{-1}$ injection rates show quite improper gas quality; in addition, almost all the produced gas after 100 d is CO_2, due to channeling phenomena.

Table 6 provides the results, which show that the total shale gas production increases at first with increasing CO_2 injection rate; the total shale gas production then shows a decrease after reaching a maximum value. When the injection rate is too high, it is observed that the total shale gas production is even smaller than the production without injection. This is due to the CO_2 breakthrough, which is created by excessive CO_2 injection. Large amounts of CO_2 can create tunnels to the hydraulic fractures and production wells. Then CO_2

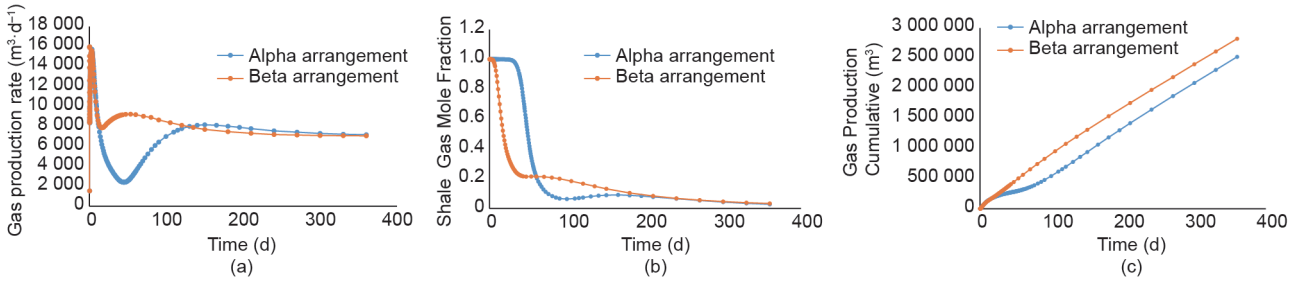

Fig. 7. (a) Gas production rate for different well arrangements; (b) shale gas mole fraction for different well arrangements; (c) total gas production for different well arrangements.

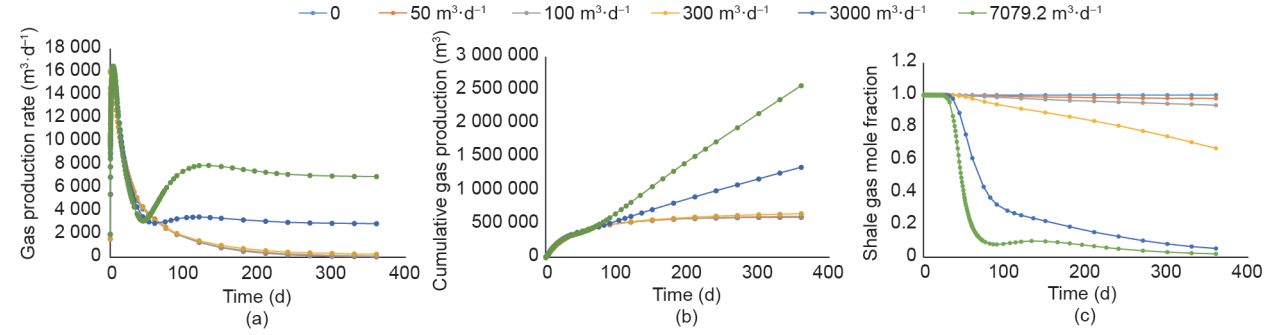

Fig. 8. (a) Gas production rate for different CO_2 injection rates; (b) total gas production for different CO_2 injection rates; (c) shale gas mole fraction for different CO_2 injection rates.

can flow into the production wells directly, without pushing the shale gas in the matrix; rather, it impedes the shale gas from entering the production wells. In other words, too-large or too-small injection rates will either sabotage the gas production or have little effect. There is an optimal CO_2 injection rate that can obtain maximum shale gas production.

Table 6
Total shale gas production for different CO_2 injection rates.

Case	CO_2 injection rate ($m^3 \cdot d^{-1}$)	Total shale gas production (m^3)
1	0	600 450
2	50	607 400
3	100	611 320
4	300	608 800
5	3000	603 000
6	7079.2	541 250

The costs of CO_2 injection and of drilling the injection wells are critical economic factors that should be taken into account. The economic benefits of the cases with CO_2 injection should be quantified in terms of the NPVs. Table 7 displays the sensitivity of the NPVs with respect to CO_2 price, shale gas price, and tax rate, for different injection rates. For example, for Scenarios 1–5, the tax rate is 30%, and the shale gas price is 0.319 USD·m^{-3} (9.5 USD·MMBtu^{-1}, assuming 950 Btu·ft^{-3} for the heating value of shale gas). The sensitivity is applied with respect to the price of CO_2. This analysis suggests that if the CO_2 price decreases by 50%, the NPV becomes positive. However, due to the low price of shale gas, the scenario with no CO_2 injection performs economically better, even for such cheap CO_2 streams. Two prospective sets of scenarios can promote the sequestration of CO_2 in shale gas reservoirs. Firstly, the depletion of conventional energy resources can increase the price of shale gas. Secondly, governments

Table 7
NPV of shale gas production for different cases shown in Table 6.

Scenario	Tax rate	CO_2 price (USD·m^{-3})	Shale gas price (USD·m^{-3})	Price ratio	NPV (USD)					
					Case 1	Case 2	Case 3	Case 4	Case 5	Case 6
1	30%	1.450	0.319	4.550	21 563	−2 986	−28 212	−133 174	−1 543 868	−3 686 883
2	30%	0.725	0.319	2.275	21 563	10 064	−2 112	−54 874	−760 868	−1 839 264
3	30%	0.363	0.319	1.137	21 563	16 589	10 938	−15 724	−369 368	−915 454
4	30%	0.181	0.319	0.569	21 563	19 851	17 463	3 851	−173 618	−453 549
5	30%	0.091	0.319	0.284	21 563	21 482	20 726	13 638	−75 743	−222 597
6	30%	1.450	0.637	2.275	155 524	132 525	108 174	2 650	−1 409 338	−3 566 129
7	30%	0.725	0.637	1.137	155 524	145 575	134 274	80 950	−626 338	−1 718 510
8	30%	0.363	0.637	0.569	155 524	152 100	147 324	120 100	−234 838	−794 701
9	30%	0.181	0.637	0.284	155 524	155 362	153 849	139 675	−39 088	−332 796
10	30%	0.091	0.637	0.142	155 524	156 994	157 111	149 462	58 787	−101 844
11	30%	1.450	3.187	0.455	1 227 210	1 216 615	1 199 261	1 089 239	−333 101	−2 600 104
12	30%	0.725	3.187	0.227	1 227 210	1 229 665	1 225 361	1 167 539	449 899	−752 485
13	30%	0.363	3.187	0.114	1 227 210	1 236 190	1 238 411	1 206 689	841 399	171 325
14	30%	0.181	3.187	0.057	1 227 210	1 239 453	1 244 936	1 226 264	1 037 149	633 230
15	30%	0.091	3.187	0.028	1 227 210	1 241 084	1 248 198	1 236 051	1 135 024	864 182
16	20%	1.450	0.319	4.550	21 563[a]	16 372	−8 728	−113 771	−1 524 650	−3 669 632
17	20%	0.725	0.319	2.275	21 563[a]	29 422	17 372	−35 471	−741 650	−1 822 013
18	20%	0.363	0.319	1.137	21 563[a]	35 947	30 422	3 679	−350 150	−898 204
19	20%	0.181	0.319	0.569	21 563[a]	39 210	36 947	23 254	−154 400	−436 299
20	20%	0.091	0.319	0.284	21 563[a]	40 841	40 209	33 042	−56 525	−205 346
21	10%	1.450	0.319	4.550	21 563[a]	35 731	10 756	−94 367	−1 505 431	−3 652 382
22	10%	0.725	0.319	2.275	21 563[a]	48 781	36 856	−16 067	−722 431	−1 804 763
23	10%	0.363	0.319	1.137	21 563[a]	55 306	49 906	23 083	−330 931	−880 953
24	10%	0.181	0.319	0.569	21 563[a]	58 569	56 431	42 658	−135 181	−419 048
25	10%	0.091	0.319	0.284	21 563[a]	60 200	59 693	52 445	−37 306	−188 096
26	5%	1.450	0.319	4.550	21 563[a]	45 410	20 497	−84 666	−1 495 822	−3 643 756
27	5%	0.725	0.319	2.275	21 563[a]	58 460	46 597	−6 366	−712 822	−1 796 137
28	5%	0.363	0.319	1.137	21 563[a]	64 985	59 647	32 784	−321 322	−872 328
29	5%	0.181	0.319	0.569	21 563[a]	68 248	66 172	52 359	−125 572	−410 423
30	5%	0.091	0.319	0.284	21 563[a]	69 879	69 435	62 147	−27 697	−179 471
31	0%	1.450	0.319	4.550	21 563[a]	55 090	30 239	−74 964	−1 486 212	−3 635 131
32	0%	0.725	0.319	2.275	21 563[a]	68 140	56 339	−3 336	−703 212	−1 787 512
33	0%	0.363	0.319	1.137	21 563[a]	74 665	69 389	42 486	−311 712	−863 703
34	0%	0.181	0.319	0.569	21 563[a]	77 927	75 914	62 061	−115 962	−401 798
35	0%	0.091	0.319	0.284	21 563[a]	79 559	79 177	71 849	−18 087	−170 846

Yellow cells refer to scenarios with no CO_2 injection. Orange cells are the scenarios with negative NPV. Green cells are more profitable compared with the corresponding yellow scenarios. Blue cells indicate other positive NPC scenarios.

[a] Tax rate is fixed at 30%, when CO_2 sequestration is not planned.

may consider incentives or tax abatements in order to encourage CO_2 sequestration. These alternatives are covered in Scenarios 16–35.

In Scenarios 6–10, the price of shale gas is two times higher, and in Scenarios 11–15, it is 10 times higher. Table 7 suggests that the NPV increases sharply as the ratio of the CO_2 price to shale gas price decreases. However, it is only for price ratios of 20% or lower that CO_2 injection can create added value and will be commercially viable.

In Scenarios 16–20, 21–25, 26–30, and 31–35, the tax rate is decreased to 20%, 10%, 5%, and 0%, respectively. Table 7 suggests that NPV is commercially competitive for almost all price ratios, starting from the price ratio of 227% for 20% tax (Scenario 17), or even the price ratio of 455% for the 10% tax ratio (Scenario 21). This observation suggests that government incentives play an important role in the commercialization of CO_2 sequestration in shale gas reservoirs.

3.2.2. Shut-in operation

The pressure of the reservoir drops continuously during the production operations, and liquid loading may occur when the pressure is very low. Consequently, the pressure gradient may not be strong enough to lift the liquids, resulting in choking and production interruption. Shut-in operation is an effective way to prevent liquid loading and enhance gas production. Shut-in scheduling and duration are important operational decisions that can influence shale gas production. In this study, three aspects of shut-in operation were investigated: the shut-in duration, the time at which the well is shut, and the shut-in frequency.

(1) **Shut-in duration.** To study the implications of shut-in duration, four time intervals were chosen: 5 d, 15 d, 30 d, and 60 d. The injection wells are shut on the 30th day in all cases. Each well has two fractures and even fracture distances. The production well length is 100 m and wells are in the alpha arrangement. There is no CO_2 injection in these cases.

Fig. 9(a) shows the gas production rates of different shut-in durations. The gas production rate increases to a high value when the well is shut for a period of time. This phenomenon is due to pressure buildup in the reservoir. It is also observed that the gas production rate increases with longer shut-in duration. The cumulated reservoir pressure is greater if the well is shut for a longer time; thus, a higher gas production rate can be achieved. Fig. 9(b) reveals the total gas production of shale gas for these cases. The results illustrate that shut-in operation improves gas production, and that the case with a shut-in lasting 15 d gives the greatest improvement. There is a trade-off between the added production gained after shut-in operation and the production lost during the operation. Too large shut-in durations result in a great amount of production being lost during the operation, while the extra production obtained after a shut-in operation is not significant if the duration is too small. Therefore, it is essential to keep the shut-in duration within an appropriate range and search for the duration with the highest shale gas production. Table 8 shows the NPV of shale gas production for different shut-in durations. The cases with more shale gas production also have higher economic profits. The results show that shut-in is an effective operation to increase economic benefits. Fig. 10 shows the pressure distribution of different shut-in durations before and after shut-in operation. This figure suggests that an increase in shut-in duration results in a decrease of the pressure gradient across the reservoir.

(2) **Shut-in timing.** Since the shale gas production rate changes from time to time, different timing of shut-in operations can lead to variations in gas production. Four cases are considered here: shut-in on the 15th day, 30th day, 60th day, and 90th day. Each well has two fractures with even fracture distances, and all wells are positioned in the alpha arrangement. The well length is 100 m, and no CO_2 injection is applied in these cases.

Fig. 11(a) shows the shale gas production rates of scenarios with different shut-in timing. It was observed that the gas production

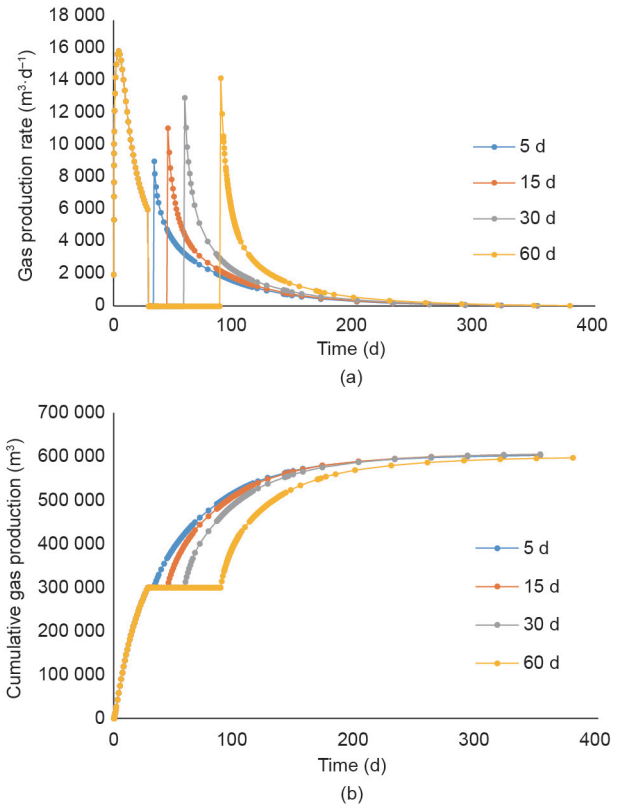

Fig. 9. (a) Shale gas production rate for different shut-in durations; (b) total gas production for different shut-in durations.

Table 8
NPV of shale gas production for different shut-in durations.

Shut-in duration (d)	NPV (USD)
5	22 295
15	22 667
30	22 423
60	21 047

rate after a shut-in rises to a higher level if the timing of the shut-in is earlier. The rise in gas production is significant when the wells are shut on the 15th day, while a shut-in on the 90th day only results in a minor increase in gas production rate. For early shut-in days, the matrix has a high capacity for shale gas production due to the high reservoir pressure. Therefore, the accumulation of released shale gas around the production well is quite large after a while, and the increase in gas production rate is significant when the well opens again. As time goes by, the pressure of the shale gas reservoir decreases, and its capacity for gas release declines. As a result, the increase in gas production rate after a shut-in is limited when the operation is applied later on.

Fig. 11(b) shows the cumulative gas production. There is an optimal timing for a shut-in operation that can lead to the greatest shale gas production. Although a shut-in results in a higher production rate afterwards if the operation is applied in the earlier days, the loss of shale gas production during the shut-in time is also greater. If the wells are shut too early, the associated production that is lost can be more significant than if they are shut later, thus reducing the increase in total shale gas production.

Table 9 gives the NPV of shale gas production for different timing of shut-in operations. The case in which wells are shut on the 30th day offers the highest economic profits. These results also suggest a direct relationship between the revenues and the total gas production.

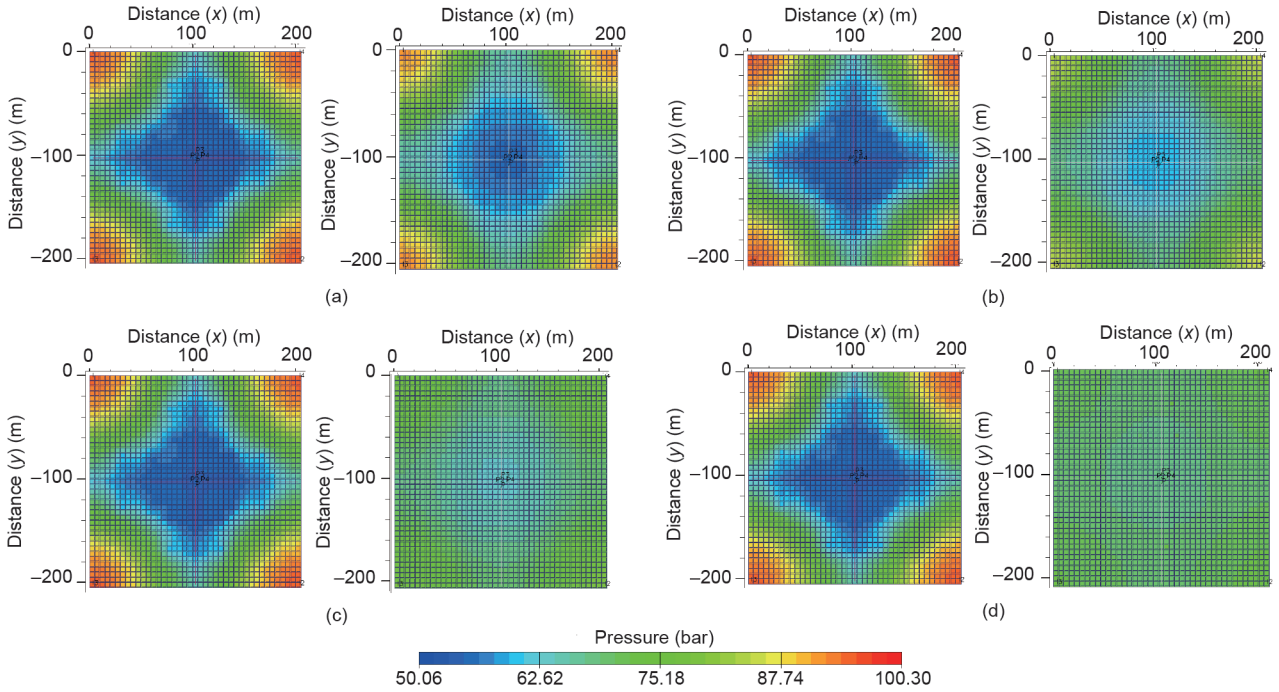

Fig. 10. Pressure distribution before (left) and after (right) shut-in operation. (a) 5 d duration; (b) 15 d duration; (c) 30 d duration; (d) 60 d duration.

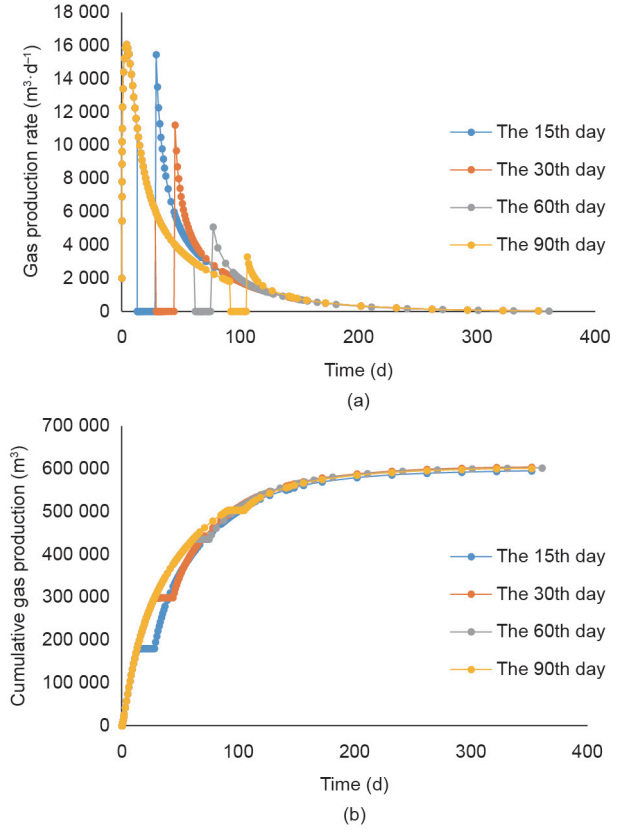

Fig.11. (a) Shale gas production rate for different timing of shut-in operations; (b) total gas production for different timing of shut-in operations.

In addition, the results reveal that all the cases with shut-in operations are more profitable than the cases without shut-in operations.

As mentioned earlier, shale gas reservoirs have significantly lower permeability than conventional gas reservoirs. The implication is that shale gas extraction results in significant pressure gradients

Table 9
NPV of shale gas production for different timing of shut-in operations.

Timing of shut-in	NPV (USD)
The 15th day	20 746
The 30th day	22 667
The 60th day	22 278
The 90th day	22 007

across the reservoir. Excessive pressure drop means that the produced gas may not be strong enough to lift the liquids, which would result in liquid loading and production interruption. A shut-in operation is an effective way to prevent liquid loading and enhance gas production. Here, a temporary shut-in of the production wells allows enough time for the sharp pressure gradient to be moderated. According to the Langmuir equation (Eq. (3)), the volume of the adsorbed gas is proportional to the reservoir pressure. Hence, a reduction in the pressure releases the adsorbed shale gas and enables its accumulation near production wells. Nonetheless, the timing of a well shut-in is a crucial decision and inherently relates to the dynamics of gas flow. If the shut-in operation is conducted too early, there may not be enough pressure gradient across the reservoir to invoke significant gas release. By comparison, if the shut-in is scheduled too late, there will again be little pressure gradient to induce gas flow.

(3) **Shut-in frequency.** Shut-in operation is an effective way to improve shale gas production rate. However, it also results in a temporary interruption in the gas extraction. In other words, conducting shut-in operations too frequently may not result in higher profits. It is crucial to schedule shut-in times properly. In this study, cases with one, two, and three shut-in operations were investigated. The shut-ins occur on the 30th day from the end of the previous shut-in operation, and the wells are shut for 15 days each time. All the wells are 100 m deep, and each well has two fractures with even distances. Wells are positioned in the alpha arrangement, and no CO_2 injection is applied in these cases.

Fig. 12(a) shows the shale gas production rate for different shut-in frequencies. When the number of shut-in operations increases,

the rise of the shale gas production rate after each operation shows a decrease. It is also observed that the increase of gas production rate after a shut-in operation is not significant when the wells have already been shut three times. Fig. 12(b) displays the total gas production for different shut-in frequencies. The results show that the most effective shut-in frequency is two times. Although the differences are small, wells that are shut three times have an even lower gas production than wells that are shut only once. This means that the third shut-in operation is unnecessary, and that the gas production lost during the shut-in interruption is greater than the additional gas that is obtained after the operation. Table 10 gives the NPV of different cases. The case with two shut-in operations has the highest economic profits. Although the third shut-in operation has a negative impact on the total gas production, the case with three shut-in operations still produces more revenue than a scenario with no shut-in operations.

3.3. An example of interaction between design and operational decisions: Number of fractures with and without shut-in operations

In Section 3.1.1, we conducted a sensitivity analysis of cases with different numbers of fractures. In this section, we add shut-in operations to all these cases in order to investigate the interactions between design and operational decisions. In each case, wells are shut once on the 15th day for a duration of 15 d. Fig. 13(a) shows the gas production rate of these cases. Cases with more fractures have a higher gas production rate at the beginning and possess a greater rise in gas production rate immediately after a shut-in operation. For the case with one fraction, it was observed that the gas production rate after a shut-in operation is significantly larger than the rate at the beginning. This phenomenon can be explained by the accumulation of shale gas around the production wells during the shut-in time. At the beginning, the pressure of the shale gas reservoir is quite high; thus, the amount of shale gas moving out of the matrix is very high. However, it takes some time for the gas in the farther regions of the matrix to move to the hydraulic fractures and production wells. If a shut-in operation is conducted shortly after the start date, the pressure drop of the shale reservoir is not significant. Therefore, the gas production rate after a shut-in operation increases sharply. Fig. 14 depicts the pressure for the case with one fracture

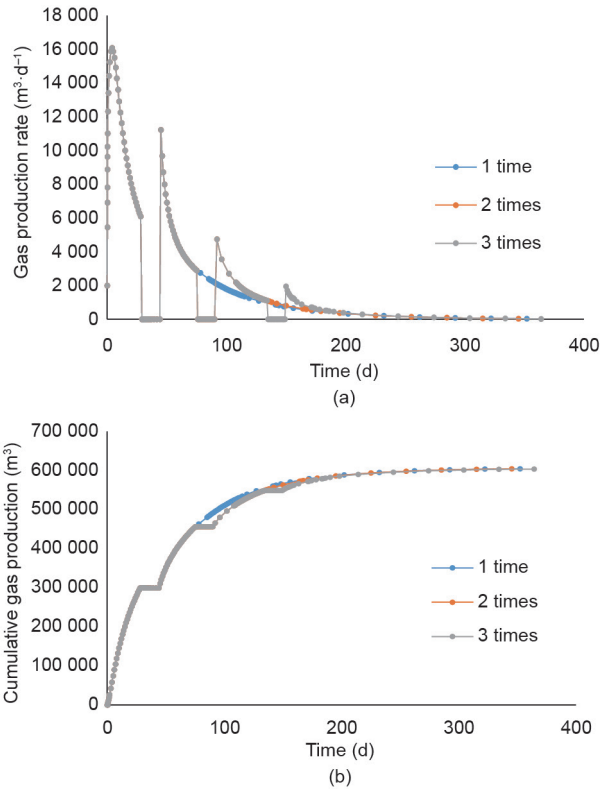

Fig. 12. (a) Shale gas production rate for different shut-in frequencies; (b) total gas production for different shut-in frequencies.

Table 10
NPV of shale gas production for different shut-in frequencies.

Shut-in frequencies	NPV (USD)
1 time	22 667
2 times	22 730
3 times	22 611

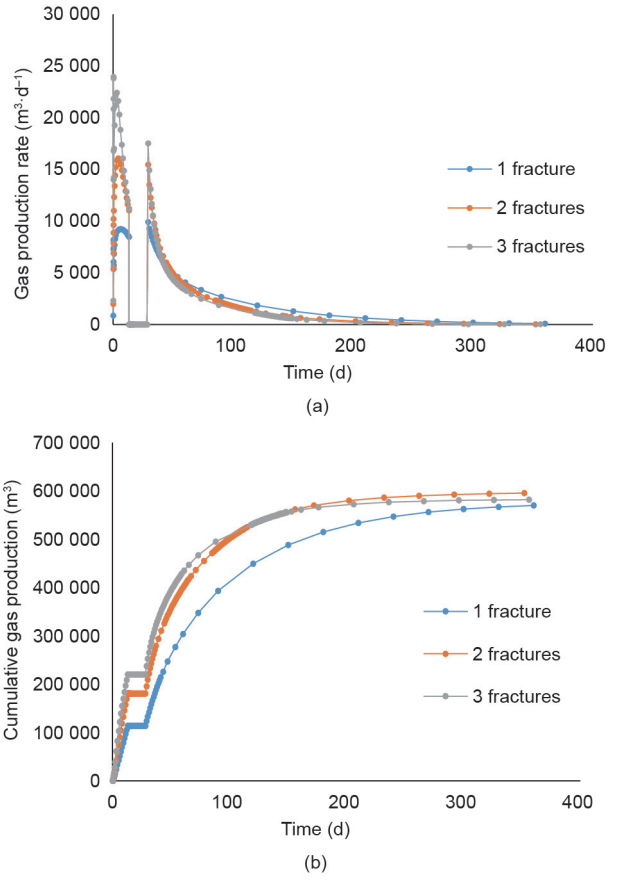

Fig. 13. (a) Shale gas production rate for different numbers of fractures (one shut-in operation on the 15th day); (b) total gas production for different numbers of fractures (one shut-in operation on the 15th day).

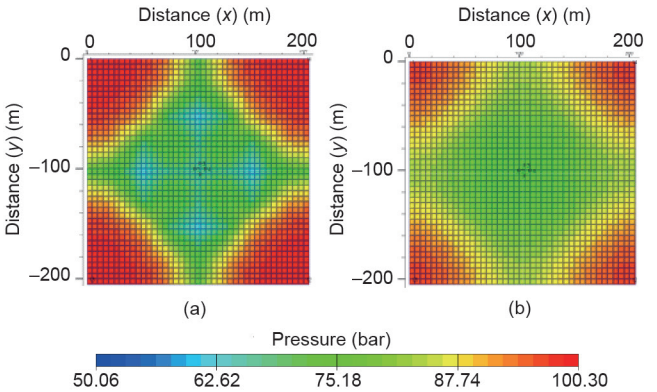

Fig. 14. Pressure map. (a) Before the shut-in operation; (b) after the shut-in operation.

before and after a shut-in operation. The pressure of the area is more homogenous after a shut-in because the gas from farther regions of the matrix has moved closer to the production wells, and there is little pressure gradient.

Fig. 13(b) shows the total gas production for these cases. The case with two fractures still has the highest shale gas production, while the case with one fracture has the lowest production. Table 11 lists detailed comparisons of the NPVs for cases with and without shut-in operations. The results show that the impact of a shut-in operation is more significant in the case with one fracture as compared with the other cases. The results of this case study demonstrate that the interactions between design and operational decisions are not negligible. Increased production and better NPV can be achieved when design and operational decisions are considered at the same time.

Table 11
Comparison of total production and NPV for different numbers of fractures, with and without shut-in operations.

Fracture number	With shut-in operations		Without shut-in operations	
	Total gas production (m^3)	NPV (USD)	Total gas production (m^3)	NPV (USD)
1	569 684	15 182	587 683	21 090
2	596 509	20 746	600 455	21 563
3	582 845	Negative	585 803	Negative

4. Discussion: Interactions between design and operational decisions

In the previous section, important decisions were analyzed. A case study was applied to discuss the interactions between design and operational decisions. It was shown that there are optimum values for fracture number, fracture distance, CO_2 injection rate, and shut-in schedules that result in maximum shale gas production and economic gains. However, the case with the most gas production may not have the greatest economic benefits. The costs of drilling, hydraulic fracturing, and CO_2 injection have a great impact on revenues. Therefore, isolated decision-making can result in economic losses. The outcomes of these decisions are influenced by each other. In order to maximize profitability and identify the optimal solution, design and operational decisions should be considered and optimized simultaneously.

5. Conclusions

In the present study, a full-physics model of a small-sized reservoir was developed and applied to study the economic performance of a shale gas network, including different arrangements of production wells and injection wells. It was observed that the economics of shale gas production are greatly influenced by the revenues generated by shale gas production and by the cost of drilling, fracturing, and CO_2 injection. Establishing two fractures on each well can result in higher gas production and revenues. It is also beneficial if the fracture distances are even. Short wells result in lower gas production but higher economic profits. This result is due to the significant cost of drilling. In the densely drilled reservoir considered here, the SRV was not large enough, so the gas production was insufficient to eliminate the impact of drilling cost. The operational strategy of CO_2 injection can potentially increase shale gas production within a certain range. However, the economic benefit can only be justified for price ratios (CO_2/shale gas) of 20% or lower. On the other hand, tax abatement policies can greatly encourage this environmentally friendly technology, even for price ratios as high as 400%. Shut-in operation is an effective way to boost gas production and economic profits. There is an optimal shut-in arrangement that can obtain the maximum revenues. Among all the cases in this study, the best shut-in arrangement has two shut-in operations spaced 30 days apart and lasting for 15 days each time. The interactions between design and operational decisions also have a great impact on shale gas production and economic profits. It is important to consider design and operational decisions simultaneously in order to obtain the globally optimal result. Overall, the sensitivity analysis conducted in this study uncovered significant optimization variables. Subject to the underlying assumptions, the NPV was most sensitive to well length and fracture distance, followed by shut-in variables such as timing and duration. Number of fractures was found to be the least important for a small-sized reservoir. It should be noted that the decision variables are highly interactive. Furthermore, there are various uncertainties in the model parameters that can influence the numerical results to some extent. We will undertake scale-up and simultaneous optimization of design and operational decisions under uncertainty in our future research.

Compliance with ethics guidelines

Sharifzadeh Mahdi, Xingzhi Wang, and Nilay Shah declare that they have no conflict of interest or financial conflicts to disclose.

References

[1] Sharifzadeh M. Integration of process design and control: A review. Chem Eng Res Des 2013;91(12):2515–49.
[2] Sharifzadeh M, Thornhill NF. Integrated design and control using a dynamic inversely controlled process model. Comput Chem Eng 2013;48:121–34.
[3] Sharifzadeh M, Meghdari M, Rashtchian D. Multi-objective design and operation of solid oxide fuel cell (SOFC) triple combined-cycle power generation systems: Integrating energy efficiency and operational safety. Appl Energy 2017;185(Part 1):345–61.
[4] Ran B, Kelkar M. Fracture stages optimization in Bakken shale formation. In: Proceedings of the 3rd Unconventional Resources Technology Conference; 2015 Jul 20–22; San Antonio, USA. San Antonio: URTeC; 2015.
[5] Balan HO, Gupta A, Georgi DT, Al-Shawaf AM. Optimization of well and hydraulic fracture spacing for tight/shale gas reservoirs. In: Proceedings of the 4rd Unconventional Resources Technology Conference; 2016 Aug 1–3; San Antonio, USA. San Antonio: URTeC; 2016.
[6] Whitson CH, Rahmawati SD, Juell A. Cyclic shut-in eliminates liquid-loading in gas wells. In: Proceedings of the SPE/EAGE European Unconventional Resources Conference and Exhibition; 2012 Mar 20–22; Vienna, Austria. Richardson: Society of Petroleum Engineers; 2012.
[7] Knudsen BR. Production optimization in shale gas reservoirs [dissertation]. Trondheim: Norwegian University of Science and Technology; 2010.
[8] Knudsen BR, Foss B, Whitson CH, Conn AR. Target-rate tracking for shale-gas multi-well pads by scheduled shut-ins. IFAC Proceedings Volumes 2012;45(15):107–13.
[9] Knudsen BR, Foss B. Shut-in based production optimization of shale-gas systems. Comput Chem Eng 2013;58:54–67.
[10] Knudsen BR, Grossmann IE, Foss B, Conn AR. Lagrangian relaxation based decomposition for well scheduling in shale-gas systems. Comput Chem Eng 2014;63:234–49.
[11] Vermylen JP. Geomechanical studies of the Barnett shale [dissertation]. California: Stanford University; 2011.
[12] Eshkalak MO, Al-Shalabi EW, Sanaei A, Aybar U, Sepehrnoori K. Simulation study on the CO_2-driven enhanced gas recovery with sequestration versus the re-fracturing treatment of horizontal wells in the U.S. unconventional shale reservoirs. J Nat Gas Sci Eng 2014;21:1015–24.
[13] Kulga B, Dilmore R, Wyatt C, Ertekin T. Investigation of CO_2 storage and enhanced gas recovery in depleted shale gas formations using a dual-porosity/dual-permeability, multiphase reservoir simulator [Internet]. Morgantown: US Department of Energy, National Energy Technology Laboratory; 2014 Sep 25 [cited 2017 Mar 10]. Available from: https://www.netl.doe.gov/File Library/Research/onsite research/publications/NETL-TRS-4-2014_CO2-Storage-and-Enhanced-Gas-Recovery_20140925.pdf.
[14] Li X, Elsworth D. Geomechanics of CO_2 enhanced shale gas recovery. J Nat Gas Sci Eng 2015;26:1607–19.
[15] Koederitz LF. Lecture notes on applied reservoir simulation. Singapore: World Scientific; 2005.
[16] Soeder DJ. Petrophysical characterization of the Marcellus & other gas shales [Internet]. 2011 Sep 28 [cited 2017 Feb 4]. Available from: http://www.thepttc.org/workshops/eastern_092811/eastern_092811_Soeder.pdf.
[17] Wang C, Wu Y. Characterizing hydraulic fractures in shale gas reservoirs using transient pressure tests. Petroleum 2015;1(2):133–8.

[18] Swami V, Clarkson CR, Settari A. Non-Darcy flow in shale nanopores: Do we have a final answer? In: Proceedings of the SPE Canadian Unconventional Resources Conference; 2012 Oct 30–Nov 1; Calgary, Canada. Richardson: Society of Petroleum Engineers; 2012.
[19] Aguilera R. Incorporating capillary pressure, pore throat aperture radii, height above free-water table, and Winland r_{35} values on Pickett plots. Am Assoc Pet Geol Bull 2002;86(4):605–24.
[20] Liu J, Qiu Z, Huang W, Luo Y, Song D. Nano-pore structure characterization of shales using gas adsorption and mercury intrusion techniques. J Chem Pharm Res 2014;6(4):850–7.
[21] Cho Y, Ozkan E, Apaydin OG. Pressure-dependent natural-fracture permeability in shale and its effect on shale-gas well production. SPE Reserv Eval Eng 2013;16(2):216–28.
[22] Ozkan E, Brown ML, Raghavan RS, Kazemi H. Comparison of fractured horizontal-well performance in conventional and unconventional reservoirs. Dermatol Surg 2009;27(8):703–8.
[23] Queipo NV, Verde AJ, Canelón J, Pintos S. Efficient global optimization for hydraulic fracturing treatment design. J Petrol Sci Eng 2002;35(3–4):151–66.
[24] Houzé O, Tauzin E, Artus V, Larsen L. The analysis of dynamic data in shale gas reservoirs—Part 1 [Internet]. 2010 Dec [cited 2017 Mar 10]. Available from: https://www.kappaeng.com/PDF/KAPPA - The Analysis of Dynamic Data in Shale Gas Reservoirs 1.pdf.
[25] Houzé O, Trin S, Tauzin E. The analysis of dynamic data in shale gas reservoirs—Part 2 [Internet]. 2010 Dec [cited 2017 Mar 10]. Available from: https://www.kappaeng.com/PDF/KAPPA - The Analysis of Dynamic Data in Shale Gas Reservoirs 2.pdf.
[26] Houzé O, Trin S, Tauzin E. The analysis of dynamic data in shale gas reservoirs—Part 3 [Internet]. 2010 Dec [cited 2017 Mar 10]. Available from: https://www.kappaeng.com/PDF/KAPPA - The Analysis of Dynamic Data in Shale Gas Reservoirs 3.pdf.
[27] Cipolla CL, Lolon EP, Erdle JC, Rubin B. Reservoir modeling in shale-gas reservoirs. SPE Reserv Eval Eng 2010;13(4):638–53.
[28] Wang L, Torres A, Xiang L, Fei X, Naido A, Wu W. A technical review on shale gas production and unconventional reservoirs modeling. Nat Resour 2015;6(3):141–51.
[29] Schlumberger. ECLIPSE technical description. Paris: Schlumberger; 2014.
[30] Wilson K. Optimization of shale resource development using reduced-physics surrogate models [dissertation]. California: Stanford University; 2012.
[31] Lake LW, Martin J, Ramsey JD, Titman S. A primer on the economics of shale gas production just how cheap is shale gas? J Appl Corp Finance 2013;25(4):87–96.
[32] Wilson K, Durlofsky LJ. Computational optimization of shale resource development using reduced-physics surrogate models. In: Proceedings of the SPE Western Regional Meeting; 2012 Mar 21–23; Bakersfield, USA. Richardson: Society of Petroleum Engineers; 2012.
[33] Allinson G, Cinar Y, Hou W, Neal PR. The costs of CO_2 transport and injection in Australia [Internet]. Canberra: Department of Resources, Energy and Tourism; 2009 Sep [cited 2017 Mar 10]. Available from: https://industry.gov.au/Energy/Documents/cei/cst/CO2Tech - The Costs of CO_2 Transport and Injection in Australia.pdf.
[34] Williams-Kovacs J, Clarkson CR. Using stochastic simulation to quantify risk and uncertainty in shale gas prospecting and development. In: Proceedings of the Canadian Unconventional Resources Conference; 2011 Nov 15–17; Calgary, Canada. Richardson: Society of Petroleum Engineers; 2011.